Proceedings of the 28th IEEE
EMBS Annual International Conference
New York City, USA, Aug 30-Sept 3, 2006

Electrical Impedance Tomography Method for Reconstruction of Biological Tissues with Continuous Plane-Stratification

M. Dolgin, Student Member, IEEE, and P. D. Einziger

***Abstract*— A novel electrical impedance tomography method is introduced for reconstruction of layered biological tissues with continuous plane-stratification. The algorithm implements the recently proposed reconstruction scheme for piecewise constant conductivity profiles, based on an improved Prony method in conjunction with Legendre polynomial expansion (LPE). It is shown that the proposed algorithm is capable of successfully reconstructing continuous conductivity profiles with moderate (WKB) slop. Features of the presented reconstruction scheme include, an inherent linearity, achieved by the linear LPE transform, a locality feature, assigning analytically to each spectral component a local electrical impedance associated with a unique location, and effective performance even in the presence of noisy measurements.**

I. INTRODUCTION

Electrical Impedance Tomography (EIT) emerged at last decades as a promising diagnostic tool [1]-[8]. In EIT, the tissue conductivity of the interior of a biological object is reconstructed via quasistatic measurements of electric currents and voltages captured on its boundaries.

The impedance imaging problem is, in general, nonlinear and ill-posed [2]. While unique reconstructions are guarantied under a variety of assumptions [3]-[4], even for the layered structures [5] studied in this paper, reconstruction algorithms [6]-[7] for arbitrary conductivity profiles (e.g., piecewise constant, etc.) may, in general, lead to unacceptable results, particularly when finite and noisy measurements are involved.

Herein, we propose a two-step linear algorithm for reconstruction of biological tissues with continuous plane-stratification. In the first step, the measured potential undergoes a linear transformation, namely, Legendre polynomial expansion (LPE). Then, the spectral components are estimated through Prony method (PM). The algorithm is based on the recently emerged reconstruction method [9], [10] for piecewise constant conductivity profiles with planar stratification. Assuming that arbitrary continuous profile can be piece by piece approximated by a constant value, the above algorithm is applied to obtain a piecewise constant approximation of the continuous profile. The algorithms' features are: (i) analytic closed-form expressions for both the direct problem Green's function and its spectral LPE content, (ii) a locality feature, assigning analytically to each spectral component a local electrical impedance associated with a unique location, and (iii) improved PM for estimation of spectral components, leading to reconstruction of the conductivity profile even in the presence of noisy measurements.

Department of Electrical Engineering, Technion - Israel Institute of Technology, Haifa, 32000, Israel
M. Dolgin tel: +972-4-8294603, email: madlena@tx.technion.ac.il
P.D. Einziger, email: einziger@ee.technion.ac.il

II. PROBLEM DEFINITION

The electromagentic fields, induced by a current source $i(\boldsymbol{r})$, are governed by Maxwell's equations. At low frequencies and small field strengths the electromagnetic properties of living tissue allow these to be simplified to the potential equation [11],[12]

$$\nabla^2\Phi(\boldsymbol{r}) + \nabla\Phi(\boldsymbol{r})\cdot\nabla\ln(\sigma) = -\frac{i(\boldsymbol{r})}{\sigma}\,. \tag{1}$$

where $\Phi(\boldsymbol{r})$ is the electric potential at the point $\boldsymbol{r} = (\rho, \theta, z)$. Considering continuous plane stratified media,

$$\sigma = \begin{cases} \sigma(z) & z \geq z_1 = 0 \\ 0 & z < 0 \end{cases}\,, \tag{2}$$

and a current point-source S (Fig. 1)

$$i(\boldsymbol{r}) = I_0\delta(\boldsymbol{r} - \boldsymbol{r}')\,, \tag{3}$$

located at the origin $\boldsymbol{r}'$, we aim to reconstruct $\sigma(z)$ in Eq. (2) for $z > 0$ using a noninvasive measurements of the potential $\Phi(\boldsymbol{r})$ at the plane $z = 0$.

III. RECONSTRUCTION ALGORITHM

Let's assume that we approximate the continuous profile by piecewise constant profile, as depicted in Fig. 2. Mathematically, we denote the approximated piecewise constant conductivity by σ_i

$$\sigma_i = \sigma(\hat{z}_i)\,, \tag{4}$$

corresponding to the i-th layer via

$$z_{i-1} < \hat{z}_i < z_i, i = 1, 2, ..., n+1, z_0 = -\infty, z_{n+1} = \infty\,. \tag{5}$$

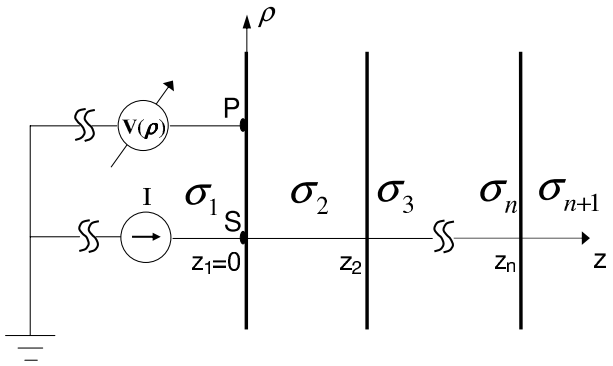

Fig. 1. Physical configuration and reconstruction setup

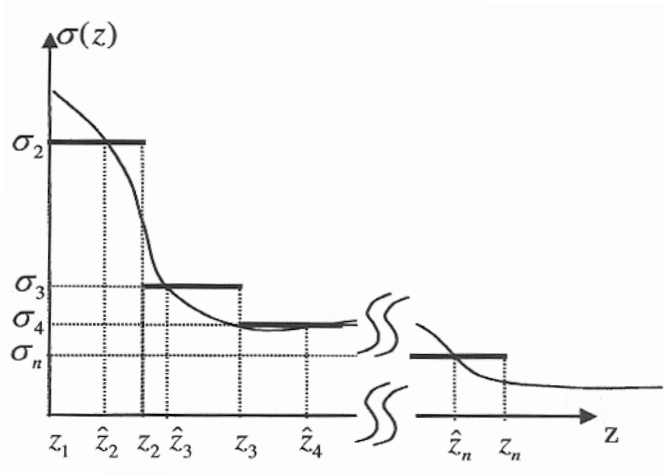

Fig. 2. Continuous profile discretization

A reconstruction procedure can now be performed by utilizing our perviously introduced [9], [10] reconstruction method, which is most effective for WKB-based [13] piecewise constant conductivity profiles. For the sake of clarity and completeness, our reconstruction method and its relevance for the reconstruction of continuous profiles are briefly outlined.

A. WKB image series

The image series expansion of the solution of (1),(3) and (4) is given by [11],

$$\Phi(\boldsymbol{r},\boldsymbol{r}') = \frac{I}{4\pi\sigma_1}\Big[\frac{1}{|\boldsymbol{r}-\boldsymbol{r}'|}+ \\ + \sum_{l_1=0}^{1}\sum_{m_1=0}^{\infty}\cdots\sum_{l_{n-1}=0}^{s_{n-2}}\sum_{m_{n-1}=0}^{\infty}\Big\{\prod_{k=1}^{n-1}\binom{s_{k-1}+1}{l_k}\binom{s_k}{m_k} \\ \times K_k^{l_k}[1-K_k^2]^{s_{k-1}-l_k+1}[-K_k]^{m_k}K_n^{m_k-l_k}\Big\}\frac{K_n}{|\boldsymbol{r}-\tilde{\boldsymbol{r}}_k'|}\Big], \tag{6}$$

where $\boldsymbol{r}$ and $\tilde{\boldsymbol{r}}_k'$, denoting the observation and the image points, are given via $\mathbf{r} = (x,y,z)$ and $\tilde{\boldsymbol{r}}_k' = (0,0,\tilde{z}_k')$, respectively, and $\tilde{z}_k' = 2\sum_{k=1}^{n-1}(s_k+1)(z_{k+1}-z_k) - z'$, $s_n = \sum_{k=1}^{n}(m_k - l_k)$, $s_0 = 0$. In the WKB limit [13], which is reasonable in the moderately varying continuous conductivity profiles, the intrinsic reflection coefficients $K_i,\ i = 2,3,\ldots,n$, given by

$$K_i = \frac{\sigma_i - \sigma_{i+1}}{\sigma_i + \sigma_{i+1}}, \quad K_0 = 0,\ \sigma_0 = \sigma_1\,, \tag{7}$$

are assumed to be sufficiently small, i.e.,

$$|K_i| \ll 1\,. \tag{8}$$

Hence, maintaining image terms of $O(|K_i|)$, taking the limit of $(1+K_1)/\sigma_1|_{\sigma_1\to 0}$ for penetration from air and notifying that both the excitation current source I and the measured potential $V(\rho)$ are confined to the plane $z = z' = 0$, where $\rho = \sqrt{x^2+y^2}$ denotes the radial distance and $V(\rho)$ is expressed, via (6), as

$$V(\rho) = \Phi_{WKB}(\mathbf{r},\mathbf{r}')|_{z=z'=0,\sigma_1=0} = \\ = \frac{I}{\pi\sigma_2}\left[\frac{1}{2\rho} + \sum_{i=2}^{n}\frac{K_i}{[\rho^2+(2z_i)^2]^{1/2}}\right]. \tag{9}$$

B. Linear transformation - Legendre expansion

Evidently, Eq. (9) contains all the information required for reconstruction of the layered media. Evaluation of an individual ith image term in (9) leads to reconstruction of K_i and z_i and, consequently, the electrical impedance $\sigma(z)$ of the entire medium (via (4) and (7)). While a standard Least Squares (LS) optimization procedure seems capable of obtaining the desired information regarding the unknown image terms, its execution for large number of images usually results in cumbersome estimations in conjunction with unacceptable computation time. Herein, we seek for an alternative procedure, which has the potential of accurately reconstructing relatively large number of layers (i.e., distinct image terms) and significantly reducing the execution time (relative to the LS procedure).

We use shifted Legendre polynomial [14] $L_l(1-2\rho^2)$, defined on a unit window width $0 \le \rho \le w,\ w = 1$ [unit length], to expand the scaled potential $V(s\rho)$ (with respect to the Legendre's unit window width $0 \le \rho \le 1$), leading to

$$V(s\rho) = \sum_{l=0}^{\infty} b_l(s) L_l(1-2\rho^2)\,, \tag{10}$$

where [16]

$$b_l(s) = 2(2l+1)\int_0^1 \rho V(s\rho)L_n(1-2\rho^2)d\rho \\ = \frac{2(2l+1)}{s^2}\int_0^s \rho V(\rho)L_n\Big(1-2(\rho/s)^2\Big)d\rho \\ = \frac{2I}{\pi s\sigma_2}\sum_{i=1}^{n}\mathcal{K}_i\left(2z_i/s+\sqrt{1+(2z_i/s)^2}\right)^{-(2l+1)}, \tag{11}$$

and s is a positive real scaling factor. Note that s can also be regarded, via the second equality in Eq. (11), as scaling factor for Legendre's unit window width $w = 1$ (with respect to a non-scaled potential $V(\rho)$). Furthermore, while for $i > 1$, $\mathcal{K}_i = K_i$, for $i = 1$, $\mathcal{K}_1 = 1/2$, and the unknown parameter is σ_2 .

C. Prony method

It is readily recognized that the individual n terms contained in the right hand-side summation of Eq. (11) may be regarded as n distinct exponentials $\left(2z_i/s+\sqrt{1+(2z_i/s)^2}\right)^{-2}$ of power l, weighted by $2I\mathcal{K}_i\left(2z_i/s+\sqrt{1+(2z_i/s)^2}\right)^{-1}/(\pi s\sigma_2)$. Hence, The PM procedure [15] exploiting $2n$ data points, i.e., $b_l(s),\ 0 \le l \le 2n-1$ or, equivalently, $2n$ inner products,

can be utilized to reconstruct n distinct exponentials and weights characterizing the stratification geometry and electrical parameters, respectively. Also, to avoid dominance of any one of the exponentials contained in the right hand-side of eq. (11) the scaling factor s should be large enough as to support the entire reconstruction range, i.e.

$$s \geq 2z_i\,, \tag{12}$$

leading to the inclusion of $V(\rho)$ well within the window $0 \leq \rho \leq s$. Note, however, that the selection $s \gg 2z_n$, results in almost linearly dependant exponentials and, thus, should be avoided.

Following the basic PM procedure, the n unknown exponentials $\left(2z_i/s + \sqrt{1+(2z_i/s)^2}\right)^{-2}$ are roots of the n order polynomial equation

$$\sum_{p=0}^{n} c_p(\mu^2)^p = 0\,, \tag{13}$$

where $c_n = 1$. Let μ_i^2 denote the ith root of (13), then,

$$\mu_i = \left(2z_i/s + \sqrt{1+(2z_i/s)^2}\right)^{-1}\,, \tag{14}$$

leading to

$$z_i = \frac{\mu_i^2 - 1}{4\mu_i}s\,. \tag{15}$$

The polynomial coefficients denoted by the vector $\mathbf{C} = [c_0, c_1, \ldots, c_{n-1}]^T$ are solution of the linear system,

$$\mathbf{AC} = \mathbf{B}\,,\ \mathbf{C} = \mathbf{A^{-1}B}\,, \tag{16}$$

where $\mathbf{A}_{j,k} = b_{j+k-1}\,,\ j,k = 0,1,\ldots,n-1$, $\mathbf{B} = -[b_n, b_{n+1}, \ldots, b_{2n-1}]^T$ and ^{T} denotes transpose operation. Finally, the weight coefficients, denoted by the vector $\mathbf{K} = 2I[\mu_1\mathcal{K}_1,\ \mu_2\mathcal{K}_2, \ldots, \mu_n\mathcal{K}_n)]^T/(\pi s\sigma_2)$, are also solution of the linear system

$$\mathbf{MK} = \mathbf{D}\,, \mathbf{K} = \mathbf{M^{-1}D} \tag{17}$$

where $M_{i,j} = (\mu_j^2)^i$ and $\mathbf{D} = [b_0, b_1, \ldots, b_{n-1}]^T$.

However, it is well known [18] that Prony method is noise prone and unstable when estimates exponentials from noisy data. Number of modifications for the method were proposed (e.g. [17],[18]), but unfortunately, in some cases, estimations provided by these algorithms still remain insufficient. Herein, to overcome noisy data, the PM procedure utilizes oversampling of the input data (e.g., [18]). The resultant "ghost" layers, are then eliminated by identifying those characterized by complex width or negligibly small intrinsic reflection coefficient.

IV. RESULTS - RECONSTRUCTION EXAMPLE

Perhaps the most elementary continuous conductivity profile $\sigma(z)$ in (2) is the linear profile expressed as

$$\sigma(z) = \begin{cases} az+b & 0 \leq z \leq z_2 \\ az_2+b & z_2 \leq z \end{cases}\,. \tag{18}$$

The corresponding potential $\Phi(\boldsymbol{r})$ in (1)-(3) at the measurements plane $z = 0$ given via Fourier-Bessel transform

$$V(\rho) = \Phi(\rho,z)|_{z=0} = \frac{I_0}{2\pi b}\int_0^\infty d\xi J_0(\xi\rho)\times$$
$$\frac{1+\frac{\left(I_0(\xi\frac{b+az_2}{a})Y_0(-j\xi b/a)-jI_0(\xi b/a)Y_0(-j\xi\frac{b+az_2}{a})\right)\sigma_3(z_2)}{\left(I_1(\xi\frac{b+az_2}{a})Y_0(-j\xi b/a)-jI_0(\xi b/a)Y_1(-j\xi\frac{b+az_2}{a})\right)\sigma_2(z_2)}}{1+\frac{\left(I_1(\xi b/a)Y_0(-j\xi\frac{b+az_2}{a})-jI_0(\xi\frac{b+az_2}{a})Y_1(-j\xi b/a)\right)\sigma_3(z_2)}{\left(I_1(\xi\frac{b+az_2}{a})Y_1(-j\xi b/a)-I_1(\xi b/a)Y_1(-j\xi\frac{b+az_2}{a})\right)\sigma_2(z_2)}}\times$$
$$\frac{jI_1(\xi\frac{b+az_2}{a})Y_0(-j\xi b/a)+I_0(\xi b/a)Y_1(-j\xi\frac{b+az_2}{a})}{I_1(\xi\frac{b+az_2}{a})Y_1(-j\xi b/a)-I_1(\xi b/a)Y_1(-j\xi\frac{b+az_2}{a})}\,, \tag{19}$$

where, $Y(x)$ and $I(x)$ denote the Bessel function of the second kind and the modified Bessel function of the first kind, respectively. Eq. (11) provides the input data for the reconstruction algorithm. In view of (4), the reconstruction algorithm provides z_i's and the estimated value of the conductivity σ_i corresponding to the ith layer, where the depth $\hat{z}_i$ is defined via

$$\hat{z}_i = 0.9(z_i + z_{i+1})/2\,. \tag{20}$$

The reconstruction results, depicted in Figs. 3-4, reveals that the proposed algorithm accurately reconstructs linear profiles. Particularly, the first portion of them (with relative error less than 1%. However, it permits considerable deviation from the real conductivity as proceeding to the interior of the body (4% for increasing conductivity and about 10% for decreasing one). This effect is further noticeable for reconstruction from noisy data, where the algorithm reconstructs only first three layers, and can not "penetrate" beyond it. The input data bases include both noiseless data sets and noisy sets [19] characterized by 60 dB signal to noise ratio (SNR), with respect to the signal $V(s\rho)$ at the endpoint of Legendre window $w = 1$ (11) and a specified scaling factor $s = 1$. SNR level of 60 dB can be experimentally maintained utilizing the readily available narrow-band low-frequency active filters.

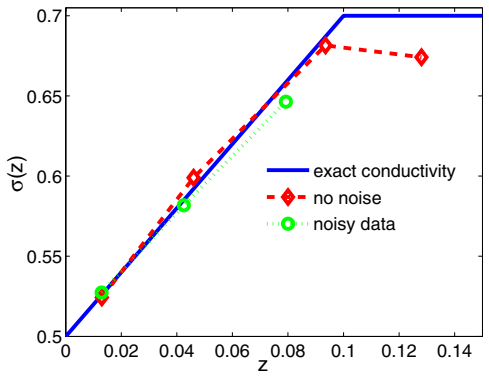

Fig. 3. Reconstruction of linearly increasing profile (18), setting: $a = 2[S/m^2], b = 0.5[S/m]$, $z_2/w = 0.1$, and $w = 1$ [unit length].

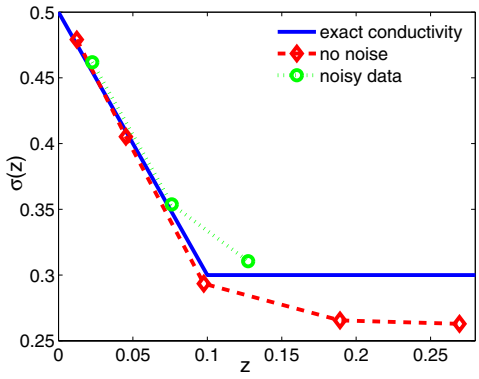

Fig. 4. Reconstruction of linearly decreasing profile (18), setting: $a = -2[S/m^2], b = 0.5[S/m]$, $z_2/w = 0.1$, and $w = 1$ [unit length].

V. CONCLUSIONS

It has readily been demonstrated that the algorithm introduced in this paper, is capable of reconstructing continuous conductivity profiles, effectively and accurately, even for noisy measurements. Although, the algorithm is based on the WKB approximation it is shown that moderate varying conductivity profiles, $0.15 < |\frac{(z_2-z_1)z\sigma'(z)}{\sigma(z_2)-\sigma(z_1)}| < 0.3$, can be reconstructed as well. The finite extent window provided by Legendre expansion allows filtering of the influence of the interior layers on the measured potential, leading to reconstruction via partial data only (no need to measure the potential on the whole boundary), at the cost of shallow reconstruction (of the first few layers only). As it is turns out, this unique feature avoids the ill-possedness usually associated with the EIT problem.

REFERENCES

[1] B. H. Brown, "Electrical Impedance Tomography (EIT): a review, *J. Medical Eng. and Tech.*, vol. 27, no. 3, pp. 97-108, 2003.

[2] D.S. Holder, Ed., *Electrical Impedance Tomography, Methods, History and Applications*, Bristol, U.K.: IOP, 2005.

[3] V. Isakov, *Inverse Problems for Partial Differential Equations*, Wichita, USA: Springer, 1998.

[4] D. Isaacson, J.L. Mueller, J.C. Newell, and S. Siltanen, "Reconstruction of Chest Phantoms by the D-Bar Method for Electrical Impedance Tomography", *IEEE Trans. Med. Imag.*, vol. 23, no. 7, pp. 821-828, 2004.

[5] R.V. Kohn and M. Vogelius, "Determining conductivity by boundary measurements II. Interior results", *Comm. on Pure and App. Math.*, vol. 38, pp. 643-667, 1985.

[6] F.C. Trigo, R. Gonzalez-Lima, and M.B.P. Amato, "Electrical Impedance Tomography Using the Extended Kalman Filter", *IEEE Trans. Med. Imag.*, vol. 51, no. 1, pp. 72-81, 2004.

[7] M. Soleimani, C.E. Powell, and N. Polydorides, "Improving the Forward Solver for the Complete Electrode Model in EIT Using Algebraic Multigrid", *IEEE Trans. Med. Imag.*, vol. 24, no. 5, pp. 577-583, 2005.

[8] S. Levy, D. Adam, and Y. Bresler, "Electromagnetic Impedance Tomography (EMIT): A New Method for Impedance Imaging", *IEEE Trans. Med. Imag.*, vol. 21, no. 6, pp. 676-87, June 2002.

[9] M. Dolgin and P.D. Einziger, "Image series expansion for electrical impedance tomography" , *Phys. Rev. Letters*, vol. 93, no. 14, Oct., 2004.

[10] M. Dolgin and P.D. Einziger, "Reconstruction of Layered Biological Tissues via Electrical Impedance Tomography" , *IEEE Trans. Biomed. Eng.* , accepted.

[11] P. D. Einziger, L. M. Livshitz, J. Mizrahi, "Rigorous image-series expansions of quasi-static Green's functions for regions with planar stratification", *IEEE Trans. Antennas Propagat.*, vol. 50, no. 12, pp. 1813-23, 2002.

[12] J.R. Wait, *Geo-Electromagnetism*, New York, Academic Press, 1982.

[13] P. M. Morse and H. Feshbach, *Methods of Theoretical Physics*, McGraw-Hill, New York, 1953.

[14] M. Abramowitz and I. A. Stegun, *Handbook of Mathematical Functions*, Dover Publications, New York, 1970.

[15] R. W. Hamming, *Numerical Methods for Scientists and Engineers*, Dover, New York, 1986.

[16] A. Erdelyi, *Tables of integral transforms*, vol. II, McGraw-Hill, New York, 1954.

[17] Y. Hua and T. P. Sarkar, "Matrix Pencil Method for Estimating Parameters of Exponentially Damped/Undamped Sinusoids in Noise", *IEEE Trans. on Acoustic, Speech and Signal Processing*, vol. 38, no. 5, pp. 814-824, May, 1990.

[18] M.R. Osborne and G.K. Smyth,"A modified Prony algorithm for exponential function fitting" , *SIAM J. Scient. Comp.*, vol. 16, no. 1, pp. 119-138, Jan., 1995.

[19] A.F. Frangi et al., "Propagation of measurement noise through back-projection reconstruction in electrical impedance tomography", *IEEE Trans. Med. Imag.*, vol. 21, no. 6, pp. 566-578, 2002.